

J functions for the process $ud \rightarrow WA$

D. Bardin¹, L. Kalinovskaya¹, E. Uglov¹, and W. von Schlippe²

¹ *Dzhelepov Laboratory for Nuclear Problems, JINR,
ul. Joliot-Curie 6, 141980 Dubna, Russia;*

² *Formerly of PNPI, RAN, Gatchina, 188300, Russia.*

Abstract

In this paper we present a description of the universal approach for analytic calculations for a certain class of J functions for six topologies of the boxes for process $ud \rightarrow WA$. These functions J arise at the reduction of infrared divergent box diagrams. The standard Passarino–Veltman reduction of four-point box diagram with an internal photon line connecting two external lines on the mass shell leads to infrared-divergent and mass-singular D_0 functions. In the system SANC a systematic procedure is adopted to separate both types of singularities into the simplest objects, namely C_0 functions. The functions J , in turn, are represented as certain linear combinations of the standard D_0 and C_0 functions. The subtracted J functions are free of both types of singularities and are expressed as explicit and compact linear combinations of dilogarithm functions. We present extensive comparisons of numerical results of SANC with those obtained with the aid of the LoopTools package.

1 Introduction

The functions J arise in the consideration of infrared divergent box diagrams. The standard Passarino–Veltman reduction [1] of the four-point box function with an internal photon line connecting two external lines on the mass shell leads to an infrared-divergent and mass-singular D_0 function.

Functions J , in turn, are represented as certain linear combinations of the standard D_0 and C_0 functions. Then the mass singularities are extracted from J to other combinations of C_0 . The rest is free of both types of singularities and are expressed as explicit and compact linear combinations of dilogarithm functions independent of the light fermion masses. The subtracted J functions, J_{sub} , have no mass singularities, and their compactness leads to stable and very fast calculations.

J functions arising in the process $f\bar{f} \rightarrow AA$ were originally described in [2]. Later on J functions for four fermion processes were considered in [3]. Within the project SANC we propose to introduce infrared finite functions J as a convenient way to disentangle the calculations.

Originally all definitions and steps of calculation for J functions in SANC were introduced in [4] for the processes $f\bar{f} \rightarrow ZZ$, $f\bar{f} \rightarrow ZA$ and $f\bar{f} \rightarrow AA$, Later on we extended our approach by introducing J functions into calculations of various channels of the process $udtb \rightarrow 0$ at EW NLO level in [5]. The explicit form the J_{sub} functions depends on the concrete channel of a process, i.e. we had no universal expression for them.

In this paper we continue the investigation of functions J and J_{sub} arising at the reduction of the infrared divergent box diagrams in the process $ud \rightarrow WA$. For this process we considered six topologies of boxes with an internal photon line.

We summarize the essential ingredients of our calculation for J functions and point to the differences with respect to [4] and [5].

We provide a universal approach for analytic calculations of expressions for J_{uni} functions valid for all six topologies for the boxes of the process $ud \rightarrow WA$.

Section 2 contains the description of the calculation of this universal function J_{uni} .

In Sections 3–5 we give our analytic results for J_{sub} for each box topology.

In Section 6 we discuss cancellations of mass singularities in the NLO EW part of the amplitude of the process under consideration.

In Section 7 we present the numerical comparison for all topologies with results obtained with the aid of the LoopTools package [6] for several values of s and $\cos\vartheta$.

In Section 8 we present our conclusions.

2 Calculation of J functions for the process $ud \rightarrow WA$

The calculation of functions J for the process $ud \rightarrow WA$ presented here closely follows the calculation of J for the channel: $ud \rightarrow tb$ presented in the Section 3 of [5] and in the earlier paper [4].

Following Section 14.10 of Ref.[3], the $ff \rightarrow bb$ boxes (f stands for a fermion, b for a boson) could be of seven types which we often call “topologies”, T_{1-7} .

For the process $ud \rightarrow WA$, we encountered six infrared divergent box diagrams giving rise to six J functions, which naturally group into three pairs:

1) T_1, T_3 , Fig. 4; 2) T_2, T_4 , Fig. 1; 3) $T_6, T_{6'}$, Fig. 7.

The basic definition of a typical function J reads (see Eq. (1)–(2) of paper [5]):

$$i\pi^2 J = \mu^{4-n} \int d^n q \frac{v(q, p_i) \cdot v(p_i)}{d_0 d_1 d_2 d_3}. \quad (1)$$

The denominators, d_0, d_1, d_2, d_3 , are the scalar parts of propagators of virtual particles that a box diagram is comprising; they are inherent to each box topology under consideration, see Sections 3–5. The numerator is the scalar product of two vectors, $v(q, p_i)$ and $v(p_i)$. These vectors must satisfy the following two properties. The first 4-vector is a linear combination of the integration vector q and of the external 4-momenta $p_{1,2,3,4}$ (ordered counter-clock-wise, see Fig. 4, and satisfying the conservation law $p_1 + p_2 + p_3 + p_4 = 0$); it is intended to cancel the infrared divergence originating from the propagator of the virtual photon. The second 4-vector, another linear combination of external 4-momenta, must be chosen in a way to simplify the subsequent integration over three Feynman parameters z, x, y , see e.g. Fig.4 and the corresponding Eqs. (38) and (41) of this paper.

The triple integral over the three Feynman parameters may be expressed by the same Eqs.(13), (16)–(17) as given in detail in paper [4]:

$$J = \int_0^1 dx \int_0^1 y dy N_{xy} \int_0^1 dz \frac{z}{(L - z k_{xy}^2)^2}, \quad (2)$$

with all the variables — N_{xy}, L and the vector squared k_{xy}^2 — being bilinear forms in Feynman parameters y, x with coefficients made of all parameters of the problem: two invariants P_1^2, P_2^2 , a selection from three Q^2, T^2, U^2 , and all the masses involved.

We recall that we use the standard SANC definitions of Mandelstam variables s, t, u

$$s = -Q^2 = -(p_1 + p_2)^2, \quad t = -T^2 = -(p_2 + p_3)^2, \quad u = -U^2 = -(p_2 + p_4)^2, \quad (3)$$

where the invariants Q^2, T^2, U^2 are given in Pauli metrics.

We omit the details of the integrations with respect to z and to x and present the integrand of the integration over y .

In Section 3.1 of paper [5] we met the case of a function J , when the variables L and k_{xy}^2 are linear in x (after one neglects a mass that does not develop a singularity). Linearity in x of the vector squared k_{xy}^2 and of the variable $L^* = L - k_{xy}^2$ is the key property which makes it possible to introduce one universal function for the calculation of all six J 's which arise in the process $ud \rightarrow WA$.

We proceed with the one-dimensional integral, see Eq.(111) of [5]:

$$J(P_1^2, P_2^2; m_1, m_2, m_3, m_4) = \int_0^1 dy I(y), \quad (4)$$

where we put the entire dummy argument list in the definition of J .

For the integrand $I(y)$ one obtains (see Eq.(112))¹ of [5]:

$$I(y) = \left(-\frac{1}{k_{xy|y}^2} - \frac{1}{T_y^2 - i\epsilon} \right) \left[\ln(L^*|_y) - \ln(P^*(1-y)) \right], \quad (5)$$

with ingredients of Eq.(113) of Ref.[5]:

$$P^* = P_1^2 + m_3^2 - i\epsilon, \quad (6)$$

$$T_y^2 = P_2^2 y(1-y) + m_1^2 y + m_4^2(1-y), \quad (7)$$

$$k_{xy|y}^2 = m_2^2 y(1-y) - m_1^2 y + P_1^2(1-y), \quad (8)$$

$$L^*|_y = -m_2^2 y(1-y) + m_1^2 y + m_3^2(1-y) - i\epsilon. \quad (9)$$

Here, as previously, $L^*|_y = L^*(x=y, y)$ and $k_{xy|y}^2 = k_{xy}^2(x=y, y)$. The differences are: change of notation $P^2 \rightarrow P^*$ and the use here of dummy invariants $P_{1,2}^2$ instead of the physical ones Q^2, T^2 which were used in [5] for a specific process.

Two sets of topologies arise in our investigation. The first one is T_2, T_4 and T_6, T_6' . For this set we received the universal answer, J_{uni} , for the integral (4) in terms of four calls to the auxiliary function of three arguments. The second set consists of two topologies T_1, T_3 . The answer for this case, J_{uni}^0 , is the limit of the previous one. It is simpler and can be expressed via three calls to a simpler auxiliary function of two arguments.

For all topologies we take the limit of vanishing light quark masses. The mass of the quark which is not coupled to the photon may be set equal to zero, while that for the quark coupled to the photon develops a mass singular logarithm. We keep quark masses in arguments of logarithmic functions and neglect them everywhere else.

¹There is a misprint in the last term of Eq.(112) of Ref.[5]; the correct one is the last term of Eq.(5) of this paper.

2.1 Result of integration over y of the first set of topologies

One can get a universal result of the integration, J_{uni} , for the first set of topologies which is expressed in terms of the auxiliary function $\mathcal{L}(a, b, c)$:

$$J_{\text{uni}}(P_1^2, P_2^2; m_1, m_2, m_3, m_4) = -\frac{1}{\sqrt{D_k}} \left(\mathcal{L}(y_{L_1^*}, y_{L_2^*}, y_{k_1}) - \mathcal{L}(y_{L_1^*}, y_{L_2^*}, y_{k_2}) \right) - \frac{1}{\sqrt{D_T}} \left(\mathcal{L}(y_{L_1^*}, y_{L_2^*}, y_{T_1}) - \mathcal{L}(y_{L_1^*}, y_{L_2^*}, y_{T_2}) \right). \quad (10)$$

The auxiliary function depends on three arguments:

$$\mathcal{L}(a, b, c) = \mathcal{M}(a, c) + \mathcal{M}(b, c) - \mathcal{M}(1, c) - \ln \left(1 - \frac{1}{c} \right) \ln \left(\frac{P^*}{m_3^2} \right), \quad (11)$$

with the ‘‘master integral’’:

$$\begin{aligned} \mathcal{M}(y_d, y_l) &= \int_0^1 \frac{dy}{(y - y_d) \ln(1 - y/y_l)} \\ &= \ln \left(1 - \frac{y_d}{y_l} \right) \ln \left(1 - \frac{1}{y_d} \right) - \text{Li}_2 \left(\frac{1 - y_d}{y_l - y_d} \right) + \text{Li}_2 \left(\frac{-y_d}{y_l - y_d} \right). \end{aligned} \quad (12)$$

The arguments of the auxiliary functions in (10) are the roots of quadratic trinomials:

- Roots of the quadratic trinomial (7):

$$y_{T_{1,2}} = \frac{-b_T \pm \sqrt{D_T}}{(-2P_2^2)}, \quad \text{where } b_T = -m_4^2 + m_1^2 + P_2^2, \quad D_T = b_T^2 + 4P_2^2(m_4^2 - i\varepsilon). \quad (13)$$

- Roots of the quadratic trinomial (8):

$$y_{k_{1,2}} = \frac{-b_k \pm \sqrt{D_k}}{(-2m_2^2)}, \quad \text{where } b_k = -m_1^2 + m_2^2 - P_1^2, \quad D_k = b_k^2 + 4m_2^2(P_1^2 + i\varepsilon). \quad (14)$$

- Roots of the quadratic trinomial (9):

$$y_{L_{1,2}^*} = \frac{-b_L \pm \sqrt{D_L}}{2m_2^2}, \quad \text{where } b_L = -m_3^2 + m_1^2 - m_2^2, \quad D_L = b_L^2 - 4m_2^2(m_3^2 - i\varepsilon). \quad (15)$$

2.2 Result of integration of the second set of topologies

This result is a particular case of the previous one (10) at $m_1 = m_3$ and $m_2 = 0$; it reads:

$$J_{\text{uni}}^0(P_1^2, P_2^2, m_3, 0, m_3, m_4) = -\frac{1}{P^*} \left[\mathcal{L}_0 \left(\frac{Q^2}{P^*} \right) \right] + \frac{1}{\sqrt{D_T}} \left[\mathcal{L}_0(y_{T_1}) - \mathcal{L}_0(y_{T_2}) \right]. \quad (16)$$

The ingredients (6)–(9) simplify considerably and in this case the auxiliary function reduces to the function of one variable $\mathcal{L}_0(a)$:

$$\mathcal{L}_0(a) = \mathcal{M}(1, a) + \ln \left(1 - \frac{1}{a} \right) \ln \left(\frac{P^*}{m_3^2} \right), \quad (17)$$

where P^* is given by Eq. (6), y_{T_1} , y_{T_2} are roots (13) of the quadratic trinomial (7) and the master integral $\mathcal{M}(y_d, y_l)$ is the same as before, Eq. (12).

3 Topologies T_2, T_4

3.1 Definition of functions J^{T_2, T_4}

For the process $u\bar{d} \rightarrow WA$, the box diagrams for the topologies T_2, T_4 are shown in Fig. 1. They are of the *direct* and *crossed* type, respectively.

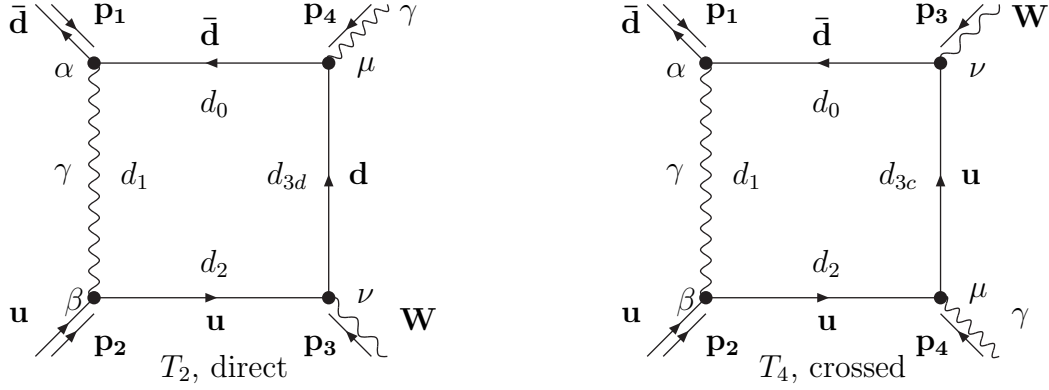


Figure 1: Process $u\bar{d} \rightarrow WA$. Box topologies T_2 and T_4 .

The direct channel function J^{T_2} is defined by the following equation:

$$i\pi^2 J^{T_2} = \mu^{4-n} \int d^n q \frac{2(q+p_1)p_4}{d_0(m_d)d_1(0)d_2(m_u)d_{3d}(m_d)}; \quad (18)$$

its arguments are not shown on purpose. The relevant masses enter through the scalar denominators d_i :

$$d_0 = q^2 + m_d^2 \quad (19)$$

$$d_1 = (q+p_1)^2 \quad (20)$$

$$d_2 = (q+p_1+p_2)^2 + m_u^2 \quad (21)$$

$$d_{3d} = (q-p_4)^2 + m_d^2 \quad (22)$$

$$d_{3c} = (q-p_3)^2 + m_u^2 \quad (23)$$

The direct function J^{T_2} is expressed via the universal function

$$J_{\text{uni}}(P_1^2, P_2^2; m_1, m_2, m_3, m_4), \quad (24)$$

given by Eq. (10) of the previous Section:

$$J^{T_2} = J_{\text{uni}}(T^2, Q^2; m_u, M_W, m_d, m_d). \quad (25)$$

For the related cross channel topology the definition of J^{T_4} looks similarly:

$$i\pi^2 J^{T_4} = \mu^{4-n} \int d^n q \frac{-2(q+p_1)p_4}{d_0(m_d)d_1(0)d_2(m_u)d_{3c}(m_u)}. \quad (26)$$

The same comment about its arguments is also valid here, and in terms of J_{uni} one gets

$$J^{T_4} = J_{\text{uni}}(U^2, Q^2; m_d, M_W, m_u, m_u). \quad (27)$$

- J^{T_2, T_4} as functions of D_0 and C_0

For topology T_2 using the standard Passarino–Veltman reduction it is possible to derive relations between infrared- and mass-singular functions

$$D_0(-m_d^2, -m_u^2, -M_W^2, 0, Q^2, T^2; m_d, 0, m_u, m_d) \text{ and } C_0(-m_d^2, -m_u^2, Q^2; m_d, 0, m_u)$$

and our infrared finite but mass-singular J -function under consideration, J^{T_2} , and another $C_0(-m_u^2, -M_W^2, T^2; 0, m_u, m_d)$ with mass singularity.

This relation, exact in all masses, is

$$\begin{aligned} J^{T_2} &= (T^2 + m_d^2) D_0(-m_d^2, -m_u^2, -M_W^2, 0, Q^2, T^2; m_d, 0, m_u, m_d) \\ &\quad - C_0(-m_d^2, -m_u^2, Q^2; m_d, 0, m_u) + C_0(-m_u^2, -M_W^2, T^2; 0, m_u, m_d). \end{aligned} \quad (28)$$

For J^{T_4} , a similar relation holds. However, neglecting terms proportional to the quark mass powers $m_{u,d}^2/Q^2$, one gets

$$\begin{aligned} J^{T_4} &= (U^2 + m_u^2) D_0(-m_d^2, -m_u^2, 0, -M_W^2, Q^2, U^2; m_d, 0, m_u, m_u) \\ &\quad - C_0(-m_d^2, -m_u^2, Q^2; m_d, 0, m_u) + C_0(-m_d^2, -M_W^2, U^2; 0, m_d, m_u). \end{aligned} \quad (29)$$

It is a typical property of such relations to be exact in masses for *direct* boxes, but for *crossed* boxes only up to some mass power terms, which we do not control anyway.

The great advantage of relations (28)–(29) is the following. The complicated object D_0 , containing an infrared divergence, is excluded in favor of explicitly computed functions J^{T_2} and J^{T_4} and the simplest infrared-divergent object $C_0(-m_d^2, -m_u^2, Q^2; m_d, 0, m_u)$, whose infrared divergences can be regularized by any method: by a photon mass, by dimensional regularization or by the width of an unstable particle. Examples of C_0 functions regularized by the width can be found in Ref. [7].

- Subtracted functions $J_{\text{sub}}^{T_2,4}$

Adding to the relations (28)–(29) the other pinches of the primary D_0 (which in general are mass-singular) with correspondingly adjusted kinematical coefficients, one gets the “subtracted functions” $J_{\text{sub}}^{T_2,4}$ which are free of quark mass singularities:

$$\begin{aligned}
J_{\text{sub}}^{T_2} &= (T^2 + m_d^2) D_0(-m_d^2, -m_u^2, -M_W^2, 0, Q^2, T^2; m_d, 0, m_u, m_d) \\
&\quad - C_0(-m_d^2, -m_u^2, Q^2; m_d, 0, m_u) - \frac{T^2}{Q^2} C_0(0, -m_d^2, T^2; m_d, m_d, 0) \\
&\quad - \frac{T^2 + M_W^2}{Q^2} C_0(-m_u^2, -M_W^2, T^2; 0, m_u, m_d) \\
&\quad - \frac{Q^2 + M_W^2}{Q^2} C_0(0, -M_W^2, Q^2; m_d, m_d, m_u), \tag{30}
\end{aligned}$$

and

$$\begin{aligned}
J_{\text{sub}}^{T_4} &= (U^2 + m_u^2) D_0(-m_d^2, -m_u^2, 0, -M_W^2, Q^2, U^2; m_d, 0, m_u, m_u) \\
&\quad - C_0(-m_d^2, -m_u^2, Q^2; m_d, 0, m_u) - \frac{U^2}{Q^2} C_0(0, -m_u^2, U^2; m_u, m_u, 0) \\
&\quad - \frac{U^2 + M_W^2}{Q^2} C_0(-m_d^2, -M_W^2, U^2; 0, m_d, m_u) \\
&\quad - \frac{Q^2 + M_W^2}{Q^2} C_0(0, -M_W^2, Q^2; m_u, m_u, m_d). \tag{31}
\end{aligned}$$

3.2 Pinches of topologies T_2 and T_4

Each box diagram contains four three-point pinches. Here we present pinch diagrams and their expressions in terms of the corresponding C_0 functions for box topologies T_2 and T_4 . Note that all four pinches contribute to the relations (30)–(31). Furthermore, we give the explicit expressions for three infrared-finite and mass-singular pinches $C_{0,1-3}^{T_2}$ in the limit $m_u = m_d = 0$, i.e. keeping these masses only in arguments of logarithmic functions.

- Topology T_2 pinches

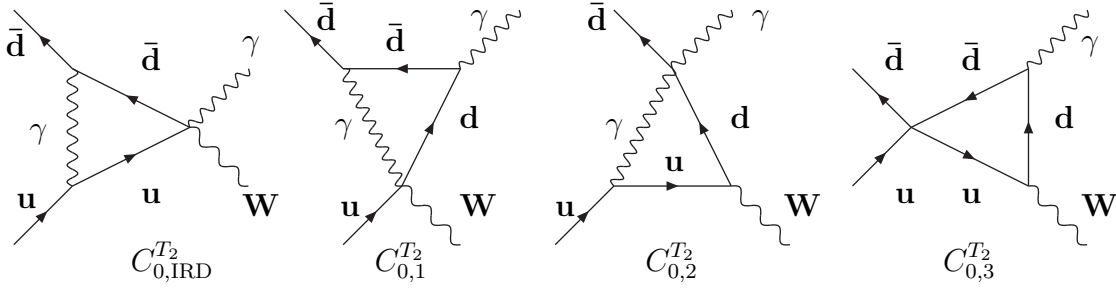


Figure 2: Diagrams of pinches for box topology T_2 .

$$\begin{aligned}
 C_{0,IRD}^{T_2} &= C_0(-m_d^2, -m_u^2, Q^2; m_d, 0, m_u), \\
 C_{0,1}^{T_2} &= C_0(0, -m_d^2, T^2; m_d, m_d, 0) = \frac{1}{T^2} \left[\frac{1}{2} \ln^2 \left(\frac{T^2 - i\varepsilon}{m_d^2} \right) + 2\zeta(2) \right], \\
 C_{0,2}^{T_2} &= C_0(-m_u^2, -M_W^2, T^2; 0, m_u, m_d) \\
 &= \frac{1}{T^2 + M_W^2} \left\{ \ln[-(1 - i\varepsilon)] \ln \left[\frac{(T^2 + M_W^2)^2 M_W^2}{(T^2)^3} \right] \right. \\
 &\quad + \text{Li}_2 \left(1 + \frac{M_W^2 - i\varepsilon}{T^2} \right) - \text{Li}_2 \left(-\frac{M_W^2 - i\varepsilon}{T^2} \right) + 4\zeta(2) \\
 &\quad \left. + \ln \left[-(1 - i\varepsilon) \frac{T^2}{M_W^2} \right] \ln \left(\frac{T^2 + M_W^2}{m_u^2} \right) - \frac{1}{2} \ln^2 \left(\frac{T^2}{M_W^2} \right) \right\}, \\
 C_{0,3}^{T_2} &= C_0(0, -M_W^2, Q^2; m_d, m_d, m_u) \\
 &= -\frac{1}{Q^2 + M_W^2} \left\{ \ln \left(-\frac{M_W^2}{Q^2} \right) \ln \left(-\frac{Q^2}{m_d^2} \right) \right.
 \end{aligned}$$

$$+\frac{1}{2} \ln\left(-\frac{M_W^2}{Q^2}\right) \left[\ln\left(\frac{M_W^2 + i\varepsilon}{Q^2}\right) - \ln(-1 + i\varepsilon) \right] \Big\}. \quad (32)$$

As is seen, for $C_{0,2}^{T_2}$ and $C_{0,3}^{T_2}$ only one quark mass (m_u and m_d , respectively) appears on the right-hand-side of the resulting expression. This means that the singularity over the other mass does not develop and may be safely neglected.

- Topology T_4 pinches

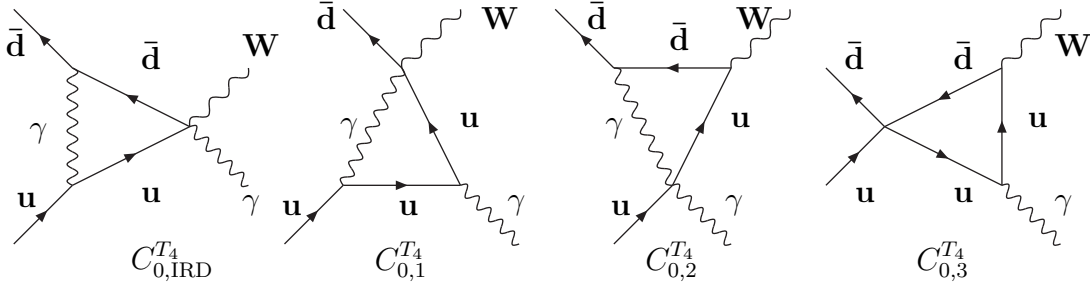


Figure 3: Diagrams of pinches for box topology T_4 .

The pinches for box topology T_4 in terms of C_0 functions are:

$$\begin{aligned} C_{0,\text{IRD}}^{T_4} &= C_0(-m_d^2, -m_u^2, Q^2; m_d, 0, m_u), \\ C_{0,1}^{T_4} &= C_0(0, -m_u^2, U^2; m_u, m_u, 0), \\ C_{0,2}^{T_4} &= C_0(-m_d^2, -M_W^2, U^2; 0, m_d, m_u), \\ C_{0,3}^{T_4} &= C_0(0, -M_W^2, Q^2; m_u, m_u, m_d). \end{aligned} \quad (33)$$

Three pinches $C_{0,1-3}^{T_4}$ are obtained from $C_{0,1-3}^{T_2}$ by the replacements $T^2 \rightarrow U^2$ and $m_d \leftrightarrow m_u$.

3.3 The final manipulations with functions $J_{\text{sub}}^{T_2, T_4}$

We exploit Eqs.(30)–(31), as well as similar expressions for the other box topologies below, in two ways. Let us exemplify this with Eqs.(28), (30) for the topology T_2 .

In the first way, we can combine the latter equations to exclude infrared divergent D_0 and C_0 and use notations (32) for pinches:

$$J_{\text{sub}}^{T_2} = J^{T_2} - \frac{T^2}{Q^2} C_{0,1}^{T_2} - \left(1 + \frac{T^2 + M_W^2}{Q^2}\right) C_{0,2}^{T_2} - \frac{Q^2 + M_W^2}{Q^2} C_{0,3}^{T_2}. \quad (34)$$

As the next step in deriving the function $J_{\text{sub}}^{T_2}$ we substitute J^{T_2} via Eq.(25) and pinches via expressions explicitly presented in the previous Section, Eqs.(32). Then the limit in the masses $m_d \rightarrow 0$ and $m_u \rightarrow 0$ is calculated. The final answer, expressed in terms of dilogarithms, does not contain logarithmic mass singularities and is very compact:

$$\begin{aligned}
J_{\text{sub}}^{T_2, T_4}(Q^2, P^2, M_W^2) &= \frac{1}{Q^2} \left[-\ln^2 \left(-\frac{M_W^2}{Q^2 + M_W^2} \right) + \ln^2 \left(\frac{M_W^2}{P^2} \right) \right. \\
&+ 2 \ln \left(-\frac{M_W^2 + i\varepsilon}{P^2} \right) \ln \left(-\frac{P^2 + M_W^2}{Q^2} \right) \\
&\left. - 2\text{Li}_2 \left(\frac{M_W^2}{Q^2 + M_W^2 + i\varepsilon} \right) + 2\text{Li}_2 \left(-\frac{M_W^2}{P^2 + i\varepsilon} \right) \right]. \quad (35)
\end{aligned}$$

Here we present the final answers for $J_{\text{sub}}^{T_2, T_4}$ for both topologies $T_{2,4}$ restoring the list of physical arguments: $P^2 = T^2$ for topology T_2 , and $P^2 = U^2$ for topology T_4 . (Note also, that for Eq. (35) we limit ourselves to the case of s-channel kinematics with $Q^2 < 0$ and $P^2 > 0$.)

In the second way, we may invert Eq.(30) to exclude the infrared divergent D_0 in favour of $J_{\text{sub}}^{T_2}$ and for $C_{0,i}^{T_2}$ pinches, $i = 1, 2, 3$. $C_{0,\text{IRD}}^{T_2}$ is assigned to the QED part of the NLO EW correction, (36), whereas $J_{\text{sub}}^{T_2}$ and the three pinches $C_{0,1-3}^{T_2}$ are assigned to the PW (Pure Weak) part of the NLO EW correction, (37):

$$\begin{aligned}
&(T^2 + m_d^2) D_0(-m_d^2, -m_u^2, -M_W^2, 0, Q^2, T^2; m_d, 0, m_u, m_d) = \\
&+ C_0(-m_d^2, -m_u^2, Q^2; m_d, 0, m_u) \quad (36)
\end{aligned}$$

$$\begin{aligned}
&- J_{\text{sub}}^{T_2}(Q^2, P^2, M_W^2) + \frac{T^2}{Q^2} C_0(0, -m_d^2, T^2; m_d, m_d, 0) \quad (37) \\
&+ \frac{T^2 + M_W^2}{Q^2} C_0(-m_u^2, -M_W^2, T^2; 0, m_u, m_d) + \frac{Q^2 + M_W^2}{Q^2} C_0(0, -M_W^2, Q^2; m_d, m_d, m_u).
\end{aligned}$$

For the box topology T_4 , its functions are treated in the same way.

4 Topologies T_1, T_3

4.1 Definition of functions J^{T_1, T_3}

For the process $u\bar{d} \rightarrow WA$, the box diagrams for the topologies T_1, T_3 are shown in Fig. 4. Like topologies T_2, T_4 they are of *direct* and *crossed* type.

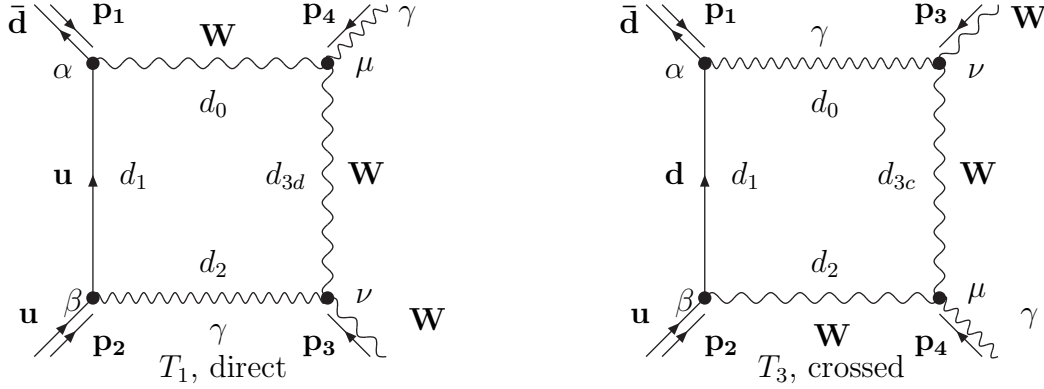


Figure 4: Process $u\bar{d} \rightarrow WA$. Box topologies T_1 and T_3 .

For the defining function J^{T_1} , we have:

$$i\pi^2 J^{T_1} = \mu^{4-n} \int d^n q \frac{2(q + p_1 + p_2)p_1}{d_0(M_W)d_1(m_u)d_2(0)d_{3d}(M_W)}. \quad (38)$$

Due to occurrence of the photon mass, $m_\gamma = 0$, in the argument list of the expression for J_{uni} , Eq.(10) fails, and a special limit

$$J_{\text{uni}}^0(P_1^2, P_2^2; m_1, 0, m_3, m_4) = \lim_{m_2 \rightarrow 0} J_{\text{uni}}(P_1^2, P_2^2; m_1, m_2, m_3, m_4) \quad (39)$$

has to be used instead. This is given by Eq. (16).

For the direct function J^{T_1} the list of arguments of the universal function J_{uni}^0 looks as follows:

$$J^{T_1} = J_{\text{uni}}^0(Q^2, T^2; M_W, 0, M_W, m_u). \quad (40)$$

For the cross channel topology T_3 the defining expression is:

$$i\pi^2 J^{T_3} = \mu^{4-n} \int d^n q \frac{-2qp_2}{d_0(0)d_1(m_d)d_2(M_W)d_{3c}(M_W)}, \quad (41)$$

and in terms of J_{uni}^0 we have:

$$J^{T_3} = J_{\text{uni}}^0(Q^2, U^2; M_W, 0, M_W, m_d). \quad (42)$$

- J^{T_1, T_3} as function of D_0 and C_0

Performing the standard PV reduction, we express J^{T_1, T_3} in terms of the corresponding D_0 and C_0 functions:

$$\begin{aligned} J^{T_1} &= (Q^2 + M_W^2) D_0(-m_d^2, -m_u^2, -M_W^2, 0, Q^2, T^2; M_W, m_u, 0, M_W) \\ &\quad - C_0(-m_u^2, -M_W^2, T^2; m_u, 0, M_W) + C_0(-M_W^2, 0, Q^2; 0, M_W, M_W), \end{aligned} \quad (43)$$

and

$$\begin{aligned} J^{T_3} &= (Q^2 + M_W^2) D_0(-m_d^2, -m_u^2, -M_W^2, 0, Q^2, U^2; M_W, m_u, 0, M_W) \\ &\quad - C_0(-M_W^2, -m_d^2, U^2; M_W, 0, m_d) + C_0(0, -M_W^2, Q^2; M_W, M_W, 0). \end{aligned} \quad (44)$$

Again, relation (43) holds exact in all masses involved, while relation (44) holds only up to quark mass power terms, $m_{u,d}^2/Q^2$, which we neglect.

- Subtracted functions $J_{\text{sub}}^{T_{1,3}}$

Only one additional pinch has to be added to the relations (43)–(44) in order to cancel remaining mass singularities:

$$\begin{aligned} J_{\text{sub}}^{T_1} &= (Q^2 + M_W^2) D_0(-m_d^2, -m_u^2, -M_W^2, 0, Q^2, T^2; M_W, m_u, 0, M_W) \\ &\quad - C_0(-m_u^2, -M_W^2, T^2; m_u, 0, M_W) + C_0(-M_W^2, 0, Q^2; 0, M_W, M_W) \\ &\quad - \frac{Q^2}{T^2 + M_W^2} C_0(-m_u^2, -m_d^2, Q^2; 0, m_u, M_W), \end{aligned} \quad (45)$$

and

$$\begin{aligned} J_{\text{sub}}^{T_3} &= (Q^2 + M_W^2) D_0(-m_d^2, -m_u^2, 0, -M_W^2, Q^2, U^2; 0, m_d, M_W, M_W) \\ &\quad - C_0(-M_W^2, -m_d^2, U^2; M_W, 0, m_d) + C_0(0, -M_W^2, Q^2; M_W, M_W, 0) \\ &\quad - \frac{Q^2}{U^2 + M_W^2} C_0(-m_u^2, -m_d^2, Q^2; M_W, m_d, 0). \end{aligned} \quad (46)$$

4.2 Pinches of topologies T_1 and T_3

For topologies T_1 and T_3 we show only those three pinch diagrams which enter in the expressions (45)–(46) and give the explicit expressions for only one infrared-finite and mass-singular

pinch $C_{0,2}^{T_1}$. The function $C_{0,1}^{T_1}$ is infrared and mass regular.

- Topology T_1 pinches

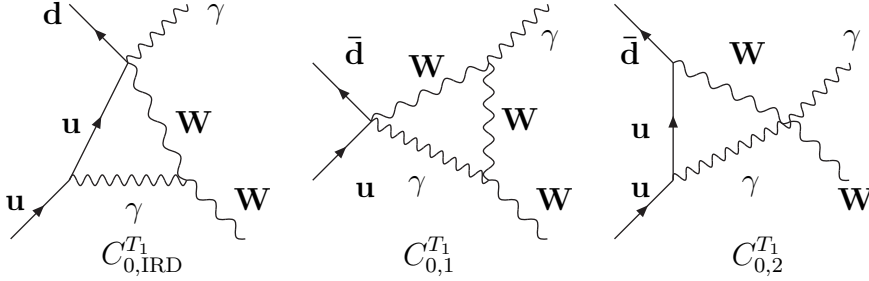


Figure 5: Diagrams of pinches for box topology T_1 .

$$\begin{aligned}
C_{0,IRD}^{T_1} &= C_0(-m_u^2, -M_W^2, T^2; m_u, 0, M_W), \\
C_{0,1}^{T_1} &= C_0(-M_W^2, 0, Q^2; 0, M_W, M_W), \\
C_{0,2}^{T_1} &= C_0(-m_u^2, -m_d^2, Q^2; 0, m_u, M_W) \\
&= \frac{1}{Q^2} \left[\ln \left(\frac{-Q^2}{M_W^2} \right) \ln \left(\frac{Q^2 + M_W^2 - i\varepsilon}{M_W^2} \right) + \text{Li}_2 \left(\frac{Q^2 + M_W^2 - i\varepsilon}{M_W^2} \right) - \zeta(2) \right]. \quad (47)
\end{aligned}$$

- Topology T_3 pinches

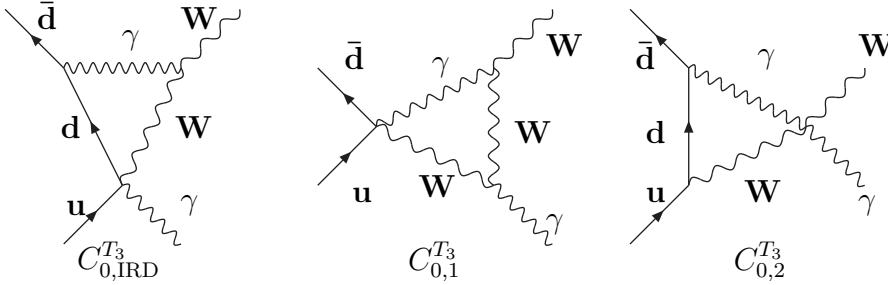


Figure 6: Diagrams of pinches for box topology T_3 .

$$\begin{aligned}
C_{0,IRD}^{T_3} &= C_0(-M_W^2, -m_d^2, U^2; M_W, 0, m_d), \\
C_{0,1}^{T_3} &= C_0(0, -M_W^2, Q^2; M_W, M_W, 0), \\
C_{0,2}^{T_3} &= C_0(-m_u^2, -m_d^2, Q^2; M_W, m_d, 0). \quad (48)
\end{aligned}$$

The explicit expression for pinch $C_2^{T_3}$ is obtained from $C_2^{T_1}$ by the replacements $T^2 \rightarrow U^2$ and $m_d \leftrightarrow m_u$.

4.3 The final manipulations with functions $J_{\text{sub}}^{T_1, T_3}$

Here the same argumentation applies as at the beginning of Section 3.3, but now for functions $J_{\text{sub}}^{T_1, T_3}$. Here we have only one mass-singular pinch $C_{0,2}^{T_1, T_3}$, (47), (48), and the equation, analogous to (34), reads:

$$J_{\text{sub}}^{T_{1,3}} = J^{T_{1,3}} - \frac{Q^2}{T^2 + M_w^2} C_{0,2}^{T_{1,3}}. \quad (49)$$

The functions J^{T_1, T_3} and $C_{0,2}^{T_1, T_3}$ are substituted, the limits in the masses $m_d \rightarrow 0$ and $m_u \rightarrow 0$ are calculated, and we arrive at a rather compact answer:

$$\begin{aligned} J_{\text{sub}}^{T_1, T_3}(Q^2, P^2, M_w^2) = & \frac{1}{Q^2 + M_w^2} \left[-\text{Li}_2 \left(-\frac{Q^2}{M_w^2 - i\varepsilon} \right) + \zeta(2) \right] \\ & + \frac{1}{P^2 + M_w^2} \left\{ \ln \left(-\frac{M_w^2 - i\varepsilon}{P^2} \right) \ln \left(\frac{P^2 + M_w^2}{M_w^2} \right) \right. \\ & + 2 \ln \left(\frac{Q^2 + M_w^2 - i\varepsilon}{M_w^2} \right) \ln \left(\frac{P^2 + M_w^2}{M_w^2} \right) \\ & - \ln \left(\frac{Q^2 + M_w^2 - i\varepsilon}{M_w^2} \right) \ln \left(\frac{-Q^2}{M_w^2} \right) \\ & \left. - \text{Li}_2 \left(\frac{Q^2 + M_w^2 - i\varepsilon}{M_w^2} \right) - \text{Li}_2 \left(\frac{P^2 + M_w^2}{M_w^2 - i\varepsilon} \right) + \zeta(2) \right\}. \quad (50) \end{aligned}$$

Here again the list of physical arguments is restored and $P^2 = T^2$ for topology T_1 and $P^2 = U^2$ for topology T_3 . Similarly to Eq. (35) we limit ourselves to the s -channel kinematics – where $Q^2 < 0$ and $P^2 > 0$ – by presenting the final expression Eq. (50).

On the other hand, one may invert Eqs.(45) and (46) in order to get rid of the infrared divergent D_0 , followed by redistribution of C_0 's as described at the end of Section 3.3.

5 Topologies $T_6, T_{6'}$

5.1 Definition of functions $J^{T_6, T_{6'}}$

For the process $u\bar{d} \rightarrow WA$, the box diagrams for the topologies $T_6, T_{6'}$ are shown in Fig. 7. They both are of *direct* type (differing only by interchange of virtual $\gamma \leftrightarrow W$) and hence relations of the type (28) and (43) will hold exactly in all masses.

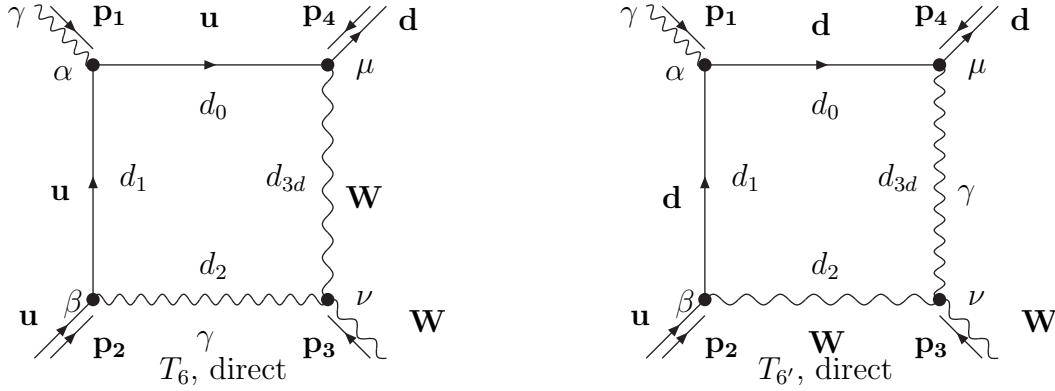


Figure 7: Process $u\bar{d} \rightarrow WA$. Box topologies T_6 and $T_{6'}$.

For the defining function J^{T_6} , we have:

$$i\pi^2 J^{T_6} = \mu^{4-n} \int d^n q \frac{2(q + p_1 + p_2)p_1}{d_0(m_u)d_1(m_u)d_2(0)d_{3d}(M_W)}. \quad (51)$$

The function J^{T_6} is expressed via the universal function J_{uni}^0 by

$$J^{T_6} = J_{\text{uni}}(U^2, T^2; M_W, m_d, m_u, m_u). \quad (52)$$

For $J^{T_{6'}}$, the pair of equations (51)–(52) becomes:

$$i\pi^2 J^{T_{6'}} = \mu^{4-n} \int d^n q \frac{2(q + p_1 + p_2 + p_3)(-p_1)}{d_0(m_d)d_1(m_d)d_2(M_W)d_{3d}(0)}, \quad (53)$$

and in terms of the universal function

$$J^{T_{6'}} = J_{\text{uni}}(T^2, U^2; M_W, m_u, m_d, m_d). \quad (54)$$

- $J^{T_6, T_{6'}}$ as function of D_0 and C_0

After the standard PV reduction, the functions $J^{T_6, T_{6'}}$ are expressed in terms of the corresponding D_0 and C_0 functions by the pair of equations

$$J^{T_6} = (U^2 + m_u^2) D_0(0, -m_u^2, -M_W^2, -m_d^2, U^2, T^2; m_u, m_u, 0, M_W) - C_0(-m_u^2, -M_W^2, T^2; m_u, 0, M_W) + C_0(-M_W^2, -m_d^2, U^2; 0, M_W, m_u), \quad (55)$$

and

$$J^{T_{6'}} = (T^2 + m_d^2) D_0(0, -m_u^2, -M_W^2, -m_d^2, U^2, T^2; m_d, m_d, M_W, 0) - C_0(-M_W^2, -m_d^2, U^2; M_W, 0, m_d) + C_0(-m_u^2, -M_W^2, T^2; m_d, M_W, 0); \quad (56)$$

- Subtracted functions $J_{\text{sub}}^{T_{6,6'}}$

$$J_{\text{sub}}^{T_6} = (U^2 + m_u^2) D_0(0, -m_u^2, -M_W^2, -m_d^2, U^2, T^2; m_u, m_u, 0, M_W) - C_0(-m_u^2, -M_W^2, T^2; m_u, 0, M_W) + C_0(-M_W^2, -m_d^2, U^2; 0, M_W, m_u) - \frac{U^2}{M_W^2 + T^2} C_0(0, -m_u^2, U^2; m_u, m_u, 0) - \frac{T^2}{M_W^2 + T^2} C_0(0, -m_d^2, T^2; m_u, m_u, M_W), \quad (57)$$

and

$$J_{\text{sub}}^{T_{6'}} = (T^2 + m_d^2) D_0(0, -m_u^2, -M_W^2, -m_d^2, U^2, T^2; m_d, m_d, M_W, 0) - C_0(-M_W^2, -m_d^2, U^2; M_W, 0, m_d) + C_0(-m_u^2, -M_W^2, T^2; m_d, M_W, 0) - \frac{T^2}{M_W^2 + U^2} C_0(0, -m_d^2, T^2; m_d, m_d, 0) - \frac{U^2}{M_W^2 + U^2} C_0(0, -m_u^2, U^2; m_d, m_d, M_W). \quad (58)$$

Here again all four pinches are present in the relations (57)–(58) for the subtracted functions $J_{\text{sub}}^{T_{6,6'}}$.

5.2 Pinches of topologies T_6 and $T_{6'}$

- Topology T_6 pinches

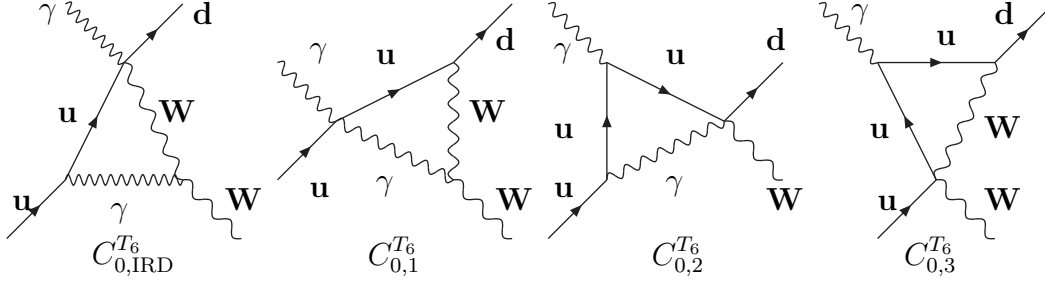


Figure 8: Diagrams of pinches for box topology T_6 .

These pinches correspond to the following C_0 functions:

$$\begin{aligned}
 C_{0,IRD}^{T_6} &= C_0(-m_u^2, -M_W^2, T^2; m_u, 0, M_W), \\
 C_{0,1}^{T_6} &= C_0(-M_W^2, -m_d^2, U^2; 0, M_W, m_u), \\
 C_{0,2}^{T_6} &= C_0(0, -m_u^2, U^2; m_u, m_u, 0), \\
 C_{0,3}^{T_6} &= C_0(0, -m_d^2, T^2; m_u, m_u, M_W) \\
 &= \frac{1}{T^2} \left[\frac{1}{2} \ln^2 \left(\frac{T^2 + M_W^2}{M_W^2} \right) + \ln \left(\frac{T^2 + M_W^2}{M_W^2} \right) \ln \left(\frac{M_W^2}{m_u^2} \right) - \text{Li}_2 \left(\frac{T^2}{T^2 + M_W^2} \right) \right]. \quad (59)
 \end{aligned}$$

The function $C_{0,1}^{T_6}$ is mass-singularity free, the explicit expression for $C_{0,2}^{T_6}$ was given above in Eqs.(32) for $C_{0,2}^{T_2}$. Here we give an explicit expression only for $C_{0,3}^{T_6}$, which was not presented so far.

- Topology $T_{6'}$ pinches

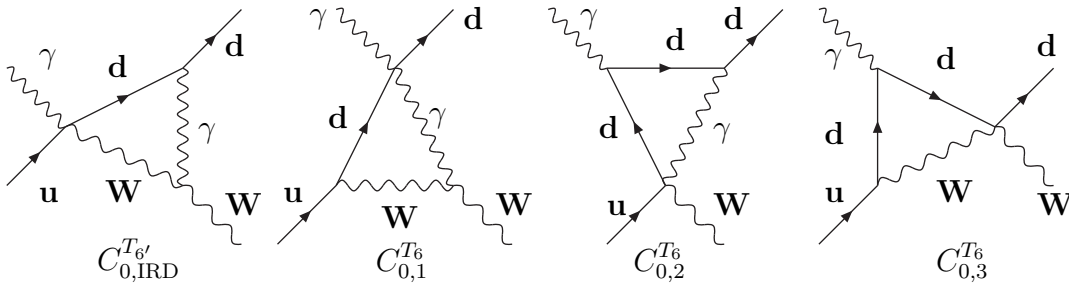


Figure 9: Diagrams of pinches for box topology $T_{6'}$.

These pinches correspond to the C_0 functions with arguments interchanged as compared to Eqs.(59):

$$\begin{aligned}
C_{0,\text{IRD}}^{T_{6'}} &= C_0(-M_W^2, -m_d^2, U^2; M_W, 0, m_d), \\
C_{0,1}^{T_{6'}} &= C_0(-m_u^2, -M_W^2, T^2; m_d, M_W, 0), \\
C_{0,2}^{T_{6'}} &= C_0(0, -m_d^2, T^2; m_d, m_d, 0), \\
C_{0,3}^{T_{6'}} &= C_0(0, -m_u^2, U^2; m_d, m_d, M_W).
\end{aligned} \tag{60}$$

The explicit expression for pinch $C_3^{T_{6'}}$ is obtained from $C_3^{T_6}$ by the replacements $T^2 \rightarrow U^2$ and $m_d \leftrightarrow m_u$.

5.3 The final manipulations with functions $J_{\text{sub}}^{T_6, T_{6'}}$

The same argumentation as in the beginning of Section 3.3 applies here. The analogue of “way one” expressions (34) and (49) in this case reads:

$$J_{\text{sub}}^{T_6} = J^{T_6} - \frac{U^2}{M_W^2 + T^2} C_{0,2}^{T_6} - \frac{T^2}{M_W^2 + T^2} C_{0,3}^{T_6}. \tag{61}$$

After substitution of its ingredients and taking the limits $m_d \rightarrow 0$ and $m_u \rightarrow 0$, we arrive at a very short answer:

$$\begin{aligned}
J_{\text{sub}}^{T_6}(T^2, U^2, M_W) &= \frac{1}{M_W^2 + U^2} \left[\frac{1}{2} \ln^2 \left(\frac{M_W^2}{U^2} \right) + 3\text{Li}_2(1) \right] \\
&+ \frac{1}{M_W^2 + T^2} \left[\frac{1}{2} \ln^2 \left(\frac{M_W^2}{U^2} \right) - \ln^2 \left(\frac{M_W^2 + T^2}{U^2} \right) - 3\text{Li}_2(1) \right].
\end{aligned} \tag{62}$$

Here the restored list of physical arguments corresponds to the topology T_6 . The answer for topology $T_{6'}$ obtains by interchange $T^2 \leftrightarrow U^2$. The expression Eq. (62) for the s -channel kinematics where $T^2 > 0$ and $U^2 > 0$ is real (has no imaginary part).

As usual, one may invert Eqs.(57) and (58) in order to exclude the infrared divergent D_0 , followed by redistribution of C_0 's as described at the end of Section 3.3.

6 Mass singularity free combinations of D_0 and C_0 functions

The “second way”, being applied to all six box topologies with a virtual photon line, eventually leads to the cancellation of many but not all mass-singular $C_{0,i}^{T_j}$ functions. The remaining mass-singular C_0 cancel after observation that certain linear combinations of D_0 (associated with boxes having a virtual Z in place of a virtual photon) and C_0 do not contain mass singularities. We verified numerically (with the aid of LoopTools) that the four following combinations converge to a stable limit when $m_u \rightarrow 0$ and/or $m_d \rightarrow 0$:

$$\begin{aligned}
C_{d_0,c_0}(Q^2, T^2) &= (Q^2 T^2 + Q^2 M_Z^2 + M_W^2 M_Z^2) \\
&\quad \times D_0(-m_d^2, -m_u^2, -M_W^2, 0, Q^2, T^2; m_d, M_Z, m_u, m_d) \\
&\quad - T^2 C_0(0, -m_d^2, T^2; m_d, m_d, M_Z) \\
&\quad - (M_W + Q^2) C_0(0, -M_W^2, Q^2; m_d, m_d, m_u); \\
C_{d_0,c_0}(Q^2, U^2) &= (Q^2 U^2 + Q^2 M_Z^2 + M_W^2 M_Z^2) \\
&\quad \times D_0(-m_d^2, -m_u^2, 0, -M_W^2, Q^2, U^2; m_d, M_Z, m_u, m_u) \\
&\quad - U^2 C_0(0, -m_u^2, U^2; m_u, m_u, M_Z) \\
&\quad - (Q^2 + M_W) C_0(0, -M_W^2, Q^2; m_u, m_u, m_d); \\
C_{d_0,c_0}(T^2, U^2) &= (T^2 U^2 + M_W^2 U^2 + M_Z^2 T^2) \\
&\quad \times D_0(0, -m_u^2, -M_W^2, -m_d^2, U^2, T^2; m_u, m_u, M_Z, M_W) \\
&\quad - U^2 C_0(0, -m_u^2, U^2; m_u, m_u, M_Z) \\
&\quad - T^2 C_0(0, -m_d^2, T^2; m_u, m_u, M_W); \\
C_{d_0,c_0}(U^2, T^2) &= (T^2 U^2 + M_W^2 U^2 + M_Z^2 T^2) \\
&\quad \times D_0(0, -m_u^2, -M_W^2, -m_d^2, U^2, T^2; m_d, m_d, M_W, M_Z) \\
&\quad - T^2 C_0(0, -m_d^2, T^2; m_d, m_d, M_Z) \\
&\quad - U^2 C_0(0, -m_u^2, U^2; m_d, m_d, M_W). \tag{63}
\end{aligned}$$

Note the nontrivial kinematical coefficients in front of the D_0 functions.

Use equations (63) to exclude four D_0 functions in favour of of the mass-singular function C_0 and of C_{d_0,c_0} which are free of mass singularities. One can verify that all 12 mass-singular C_0 functions cancel in the complete expression for the NLO PW part of the cross-section of the process under consideration, $ud \rightarrow WA$. A wonderful fact is that the mass-singular C_0 cancel as a whole, i.e. without substituting their explicit expressions.

7 Numerical Results

In this Section we compare the real and imaginary parts of the function $J_{\text{sub}}^{T_i}$, presented in Sections 3.3, 4.3 and 5.3, with the corresponding ones, computed using the LoopTools package [6].

In the Tables below, SANC results are presented in the first rows, and the corresponding LoopTools numbers in the second rows.

The numbers are given for two values of s (in GeV^2) and for three values of $\cos \vartheta$.

| $\cos \vartheta$ | $s = 10^4$ | | $s = 10^6$ | |
|------------------|-------------------|--------------------|-------------------|--------------------|
| | Re | Im | Re | Im |
| -0.999 | 6.53638473617E-08 | -1.13107515511E-07 | 3.89750326994E-11 | -3.12226209474E-09 |
| | 6.53638447452E-08 | -1.13107515739E-07 | 3.89750340292E-11 | -3.12226209489E-09 |
| 0 | 9.73334338213E-05 | -1.24690402239E-04 | 5.48800329682E-07 | -4.31508792787E-06 |
| | 9.73334338175E-05 | -1.24690402239E-04 | 5.48800329683E-07 | -4.31508792787E-06 |
| 0.999 | 8.28985241530E-04 | -2.80233766861E-04 | 5.40166075955E-05 | -3.12695141375E-05 |
| | 8.28985239959E-04 | -2.80233766861E-04 | 5.40166075954E-05 | -3.12695141375E-05 |

Table 1: Comparison of real and imaginary parts of function $J_{\text{sub}}^{T_2}$ between SANC and LoopTools results calculated for different values of s and $\cos \vartheta$. The mass of $M_w = 80$ GeV. For the topology T_4 the rows ± 0.999 have to be interchanged.

As is seen from Table 1, there is agreement from 7 to 12 digits for real and imaginary parts.

| $\cos \vartheta$ | $s = 10^4$ | $s = 10^6$ |
|------------------|--------------------|--------------------|
| | Re | Re |
| -0.999 | -2.86644118212E-04 | -2.43416713242E-03 |
| | -2.86644118211E-04 | -2.43416713242E-03 |
| 0 | -8.41693567906E-05 | 3.76366826830E-05 |
| | -8.41693567907E-05 | 3.76366826830E-05 |
| 0.999 | 1.40586637158E-03 | 1.12954414152E-03 |
| | 1.40586637160E-03 | 1.12954414152E-03 |

Table 2: Comparison of the real function $J_{\text{sub}}^{T_6}$ between SANC and LoopTools results calculated with different values s and $\cos \vartheta$; $M_w = 80$ GeV. For the topology $T_{6'}$ the rows ± 0.999 have to be interchanged.

As is seen from Table 2, we have again agreement within 10-12 digits for the functions $J_{\text{sub}}^{T_{6,6'}}$, which are real for topologies T_6 and $T_{6'}$.

| $\cos \vartheta$ | $s = 10^4$ | | $s = 10^6$ | |
|------------------|-------------------|-------------------|--------------------|--------------------|
| | Re | Im | Re | Im |
| -0.999 | 1.85671149365E-04 | 2.50678493204E-04 | 1.42521459789E-05 | 9.82990632508E-08 |
| | 1.85671149365E-04 | 2.50678493205E-04 | 1.42521459789E-05 | 9.82990632508E-08 |
| 0 | 2.36366656601E-04 | 3.69642886168E-04 | 3.20290753820E-05 | -6.95783750976E-06 |
| | 2.36366656601E-04 | 3.69642886168E-04 | 3.20290753820E-05 | -6.95783750976E-06 |
| 0.999 | 3.27769575491E-04 | 5.99387751646E-04 | -1.50514580606E-03 | 2.22442249799E-03 |
| | 3.27769575491E-04 | 5.99387751646E-04 | -1.50514580606E-03 | 2.22442249799E-03 |

Table 3: Comparison of real and imaginary parts of function $J_{\text{sub}}^{T_1}$ between SANC and LoopTools results calculated for different values s and $\cos \vartheta$. The mass of $M_W = 80.4$ GeV. For the topology T_3 the rows ± 0.999 have to be interchanged.

As is seen from the Table 3, there is agreement from 11 to 12 digits for real and imaginary parts for the topologies T_1 and T_3 .

The numerical comparison with the LoopTools library presented in this paper can be verified with help of the SANC software packages.

We have made a package related to the functions J_{T_i} , called JAWAudWA.F. This is available to download from the web page of project SANC [8].

8 Conclusions

In this paper we continue the study of the infrared and mass singularities emerging from 4-point function box diagrams with an internal photon line connecting two external lines on the mass shell, on the example of the process $ud \rightarrow WA$.

Here we extend our earlier investigations of the calculation of diagrams of such a class: see [3] and [4], where the general approach to this problem was originally proposed.

The approach consists of three steps. In the first step we introduce a new class of auxiliary functions J , relevant to the Passarino–Veltman reduction [1] of scalar and vector integrals. By construction, J functions are free of infrared singularities and are made sufficiently simple for subsequent integration over the three Feynman parameters z, x, y , leading to a compact explicit result in terms of dilogarithm functions. The function J , in turn, may be subjected to the standard Passarino-Veltman reduction giving linear combinations of the standard D_0 and C_0 functions, which may be used to exclude complicated infrared divergent D_0 function in favour of J function and simplest 3-point infrared divergent C_0 function.

In general, the explicit form of J function is not universal, depending on the concrete topology of the infrared divergent D_0 function of a process.

There are six different topologies of the infrared divergent box diagrams which are met in the analytic calculations of functions J for process $ud \rightarrow WA$. For this case we found a way to introduce a universal function by means of a special trick to simplify the analytic calculations, choosing two 4-vectors and Feynman parameterization in the defining expression for functions J , Eq. (1), which ensures linear dependence of the integrand of J on one of the integration variables, x , Eq. (2).

In this way, we received the expression for J in terms of the universal auxiliary function $J_{\text{uni}}(P_1^2, P_2^2; m_1, m_2, m_3, m_4)$. This allows us to obtain explicit expression for various topologies by a simple rotation of its dummy arguments. This is new compared to our previous papers on J functions.

The second step is typical for the SANC treatment of J functions: for each J_{uni} we build the corresponding subtracted J_{sub} functions free of mass singularities, which are shifted to some other set of mass singular C_0 functions. A part of the latter C_0 functions cancels at this step.

The third step consists of combining the four remaining mass singular D_0 functions with all remaining mass singular C_0 functions. These combinations C_{d_0, c_0} , Eq. (63), are again free of mass singularities, and all 12 mass singular C_0 functions of the problem cancel.

This approach leads to compact analytical results, allows one to perform stable and fast numerical calculations and avoid large numerical cancellations between separate terms.

Acknowledgements. This work is partly supported by Russian Foundation for Basic

References

- [1] G. Passarino and M. J. G. Veltman, *Nucl. Phys.* **B160** (1979) 151.
- [2] L. Brown and R. Feynman, *Phys.Rev.* **85** (1952) 231–244.
- [3] D. Y. Bardin and G. Passarino, Oxford, UK: Clarendon (1999) 685 p.
- [4] D. Y. Bardin, L. V. Kalinovskaya, and L. A. Rumyantsev, *Phys. Part. Nucl. Lett.* **6** (2009) 30–41.
- [5] D. Bardin, L. Kalinovskaya, V. Kolesnikov, and W. von Schlippe, *Phys.Atom.Nucl.* **73** (2010) 2048–2063, 0912.3893.
- [6] T. Hahn and M. Perez-Victoria, *Comput. Phys. Commun.* **118** (1999) 153–165, hep-ph/9807565.
- [7] D. Bardin *et al.*, *Phys. Part. Nucl. Lett.* **7** (2010) 128–141, 0903.1533 [hep-ph].
- [8] *Dubna* — <http://sanc.jinr.ru> (2007).